

## Improving the Efficiency of a Savonius Vertical Axis Wind Turbine using an Optimum Parameters

Hossein Fatahian\*, Hesamoddin Salarian, Jahanfar Khaleghinia, Esmaeel Fatahian

*Department of Mechanical Engineering, Nour Branch, Islamic Azad University, Nour, Iran*

Keywords	Abstract
Savonius wind turbine, Tip speed ratio, Overlap ratio, Power coefficient, Blade angular position.	In this study, the effect of both overlap ratio of blades and blade angular position on the performance of a savonius vertical axis wind turbine are investigated with computational fluids dynamics method. The computations are conducted for the wind turbine with overlap ratios of 0, 0.1 and 0.2. Also, the blade angular position varies from $0^\circ$ to $90^\circ$ . The results show that the optimum values for the power coefficient occurs when the tip speed ratio ranges as $0.75 \leq \lambda \leq 1.15$ . It is also concluded that the maximum value of the power coefficient and torque coefficient is obtained for overlap ratio of 0.1 for $\lambda=1$ . The highest peak of the torque coefficient is obtained at the blade angular position of $30^\circ$ for all overlap ratios. In addition, the maximum value of the power coefficient for overlap ratio of 0.1 and blade angular position of $30^\circ$ is obtained as 0.2503 when $\lambda = 1$ which is 45% more than the blade angular position of $0^\circ$ .

### 1. Introduction

Wind energy has proven to be a viable energy alternative for many of the industrialized nations according to the scientific study [1] and it is very important as one of the clean energy resources. Wind turbines are devices which convert kinetic energy of wind into rotary mechanical energy which can be used to produce electricity, charging devices and drive machinery etc. Wind turbines are the most important tool of the wind energy. Savonius wind rotor is one of the vertical axis wind turbines which is simple in structure, has good starting characteristics, relatively low operating speeds, and an ability to capture wind from any direction [2]. Savonius wind rotor was developed by a Finnish engineer, Sigurd Savonius, in 1925 [3]. Figure 1 shows the schematic view of a Savonius wind turbine and its performance mechanism.

Several studies have been undertaken for improving the performance of savonius wind turbine including the study of blade arc angle, the effect of the number of blades and blade shape coefficient. Rus [4] used a concentrator on the Savonius shaft in order to improve turbine performance. The concentrators were added to reduce the negative moments that occur on the blades. Alit et al. [5] studied the effects of adding concentrators on the performance of Savonius turbines. Their results showed that adding the concentrator could increase the power coefficient. Different geometries of Savonius wind turbine for determining the most effective operation parameters was done by Mahmoud et al. [2]. They found that the two-blade rotor is more efficient than three

and four-blade ones. They also concluded that the rotor with end plates gives higher efficiency than those without end plates. Aldoss [6] experimentally studied the aerodynamic performance of Savonius wind rotor by using a swinging blade rotor. Later, Aldoss et al. [7] developed this study and improved the performance of Savonius wind rotor by allowing the rotor blades to swing back with an optimum angle. Tabassum and Probert [8] and Reupke and Probert [9] concluded that with the Savonius wind rotor with hinged blades, higher torques could be acquired at rather lower end speeds than with the conventional Savonius wind rotors.

Ogawa et al. [10] investigated the effects on the performance of a deflecting plate which they have used to improve the performance of the Savonius wind rotor. Saha and Rajkumar [11] studied the twisted blade in a three-bladed rotor system in a low-speed wind tunnel and compared its performance with that of semicircular blades. Moreover, an experimental study with twisted blades fabricated from bamboo strips has been done by Saha et al. [12] for the small-scale power generation in rural areas. Deb et al. [13] examined the Savonius axis with a height of 60 cm and a diameter of 17 cm. The rotor model was helical Savonius with a twisted blade of  $45^\circ$ . Their results were compared to the conventional Savonius shaft. Damak et al. was also done the similar work [14]. They concluded that twisting angles of  $45^\circ$  and  $180^\circ$  produced better performances. In this study, the effect of overlap ratio (s/d) of blades and blade angular position ( $\Theta$ ) on the performance of a savonius vertical axis wind turbine are investigated with

\* Corresponding Author:

E-mail address: [fatahianhossein@gmail.com](mailto:fatahianhossein@gmail.com)– Tel, (+98) 9128430985

Received: 18 March 2018; Accepted: 28 May 2018

computational fluids dynamics method. For this purpose, the computations are conducted for the wind turbine with overlap ratios of 0, 0.1 and 0.2. Also, the blade angular position varies from 0° to 90° in order to consider the effect of these parameters on the changes of torque coefficient and power coefficient around the blades of savonius wind turbine. Then, the results of present study are compared with the experimental results of Blackwell et al. [15].

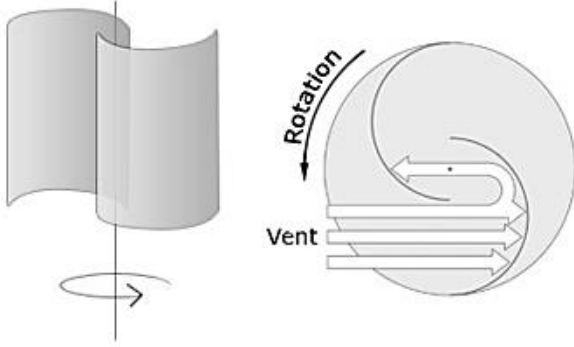


**Figure 1.** Schematic view of a Savonius wind turbine and its performance mechanism

## 2. Model Description

In this study, Ansys software is used to design the Savonius wind turbine. Figure 2 shows a 3D view of Savonius wind turbine composed in Ansys. Also, geometric characteristics of the turbine are presented in Table 1.

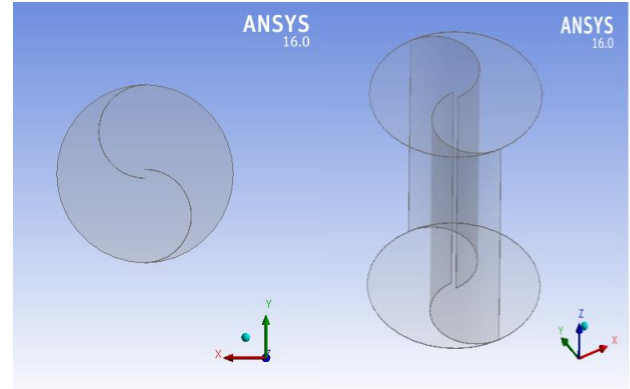


**Figure 2.** Computational domain

**Table 1.** Geometric characteristics of the turbine

Geometric characteristics	Case 1	Case 2	Case 3
Overlap ratio (s/d)	Without overlap ratio	0.1	0.2
Diameter of the blades (m)	0.5	0.5	0.5
Radius of the rotor (m)	0.5	0.475	0.45
Height of the turbine (m)	1	1	1
Diameter of the upper and lower end plates (m)	1	0.95	0.9
Thickness of the blades and end plates (m)	0.002	0.002	0.002

## 3. Governing Equation

The incompressible Reynolds-averaged Navier Stokes (RANS) equations with the shear stress transport (SST)  $k-\omega$  turbulence model are adopted to simulate the boundary layer turbulence in order to solve the air flow field around the blades of turbine. Previous studies have shown that the SST  $k-\omega$  turbulence model is a most appropriate model for simulation of wind turbine performance due to its reasonable requirement of computational resource [16-21].

Nasef et al. had studied the sensitivity in the static and dynamic performances of a Savonius rotor as the function of the RANS model. He found that SST  $k-\omega$  turbulence model is suitable for simulating the flow pattern around the Savonius rotor than other models for both stationary and rotating cases [22]. The governing equations for the air phase can be written as

Conservation equation of mass

$$\frac{\partial \rho}{\partial t} + \frac{\partial}{\partial x_i} (\rho u_i) = 0 \quad (1)$$

Conservation equation of momentum

$$\frac{\partial}{\partial t} (\rho u_i) + \frac{\partial}{\partial x_j} (\rho u_j u_i) = -\frac{\partial P}{\partial x_i} + \frac{\partial}{\partial x_j} \left[ \mu \left( \frac{\partial u_i}{\partial x_j} + \frac{\partial u_j}{\partial x_i} - \rho \overline{u'_j u'_i} \right) \right] \quad (2)$$

where  $-\rho \overline{u'_j u'_i}$  represents the Reynolds stress which is modeled by the SST  $k-\omega$  turbulence model,  $\rho$  is the air density,  $u_i$  is the air velocity component, and  $\mu$  is the air dynamic viscosity. The turbulent kinetic energy,  $k$ , and the specific dissipation rate,  $\omega$ , are obtained from the following transport equations [23].

$$\frac{\partial}{\partial t} (\rho k) + \frac{\partial}{\partial x_i} (\rho k u_i) = \frac{\partial}{\partial x_j} \left( \Gamma_k \frac{\partial k}{\partial x_j} \right) + \hat{G}_k - Y_k \quad (3)$$

$$\frac{\partial}{\partial t} (\rho \omega) + \frac{\partial}{\partial x_i} (\rho \omega u_i) = \frac{\partial}{\partial x_j} \left( \Gamma_\omega \frac{\partial \omega}{\partial x_j} \right) + G_\omega - Y_\omega + D_\omega + G_\omega - Y_\omega + D_\omega \quad (4)$$

in which,  $\Gamma_k$  and  $\Gamma_\omega$  represent the effective diffusivity of  $k$  and  $\omega$ , respectively.  $Y_k$  and  $Y_\omega$  are the dissipation of  $k$  and  $\omega$ , respectively.  $G_k$  and  $G_\omega$  represent the generation of  $k$  and  $\omega$  due to mean velocity gradients, respectively. Also,  $D_\omega$  denotes the cross-diffusion term.

The important relations for computing the parameters affecting the wind turbine performance are as follows

1. The tip speed ratio ( $\lambda$ ) of the blade is rotor radius cross the angular velocity of the rotor relative to the free air flow rate which is expressed as below [24]

$$\lambda = \frac{R\omega}{V_\infty} \quad (5)$$

2. The power coefficient,  $C_p$  represents the fraction of the available power in the wind which is extracted from the wind turbine and it is expressed as [24]

$$C_p = \frac{P}{\frac{1}{2}\rho A V_{\infty}^3} \quad (6)$$

In the above relation,  $P$  is the turbine power and  $A$  is the area swept by the turbine, which is defined as

$$A = H \times D \quad (7)$$

where,  $H$  is the blade height and  $D$  is the diameter of the turbine rotor.

3. The torque coefficient is also calculated as Eq. (8)

$$C_m = \frac{T}{\frac{1}{2}\rho A V_{\infty}^2} \quad (8)$$

In the above relation,  $T$  is the turbine torque and  $R$  represents the radius of the turbine rotor.

4. The relation between the power coefficient and torque coefficient is given by Eq. (9) [24]

$$C_p = \lambda C_m \quad (9)$$

In the present study, due to the complexity of geometry, the hexagonal meshes are used for the region of the inlet and outlet of the computational area, as well as between the blades and inside the blades. The computational domain is formed of a rectangular cube which has a 20 meters long, 12 meters wide and 12 meters height. The Savonius turbine is located at a distance of 6 meters from the entrance to the computational domain. The entire turbine is located inside a surrounded cylinder. The space between the cylinder and the wall and the space between the cylinders and the boundaries of the computational domain are separately meshed and tiny meshes are used for turbine blades. Figure 3 shows the entire grid for the entire computational domain, the inlet and outlet and around the turbine. Figure 4 shows the closer view of grids.

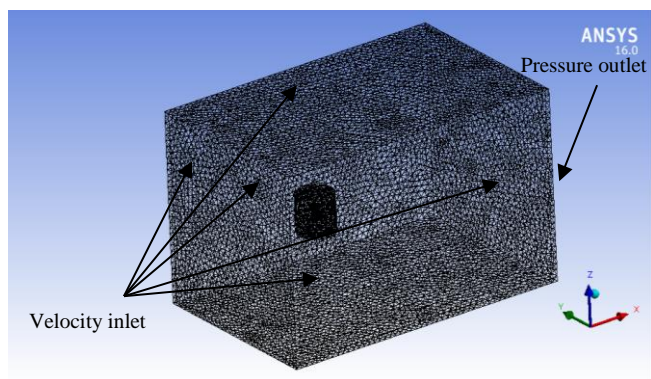


Figure 3. The entire grid

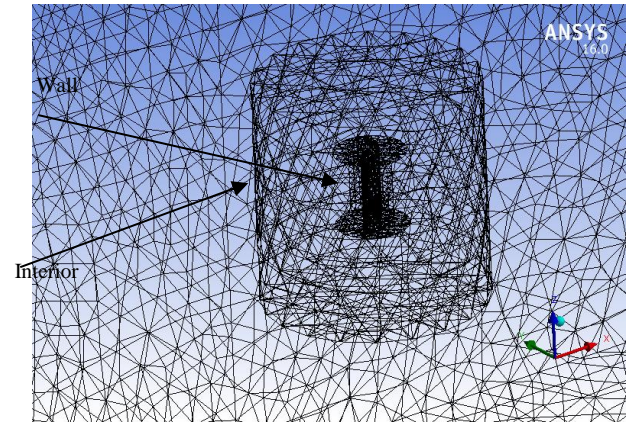


Figure 4. The closer view of grid

For the inlet side, the boundary condition is set to velocity inlet and for the outlet side the pressure outlet is set. No-slip condition is considered for entire walls. The surface of the turbine is considered as no-slip wall and the space between the turbine and the surrounded cylinder is considered as rotational zone. In this study, dynamic analysis by moving reference frames (MRF) has been used. In this method, the control volume is divided into two parts. For this purpose, a cylindrical domain has been drawn around the turbine, which is the interface between stationary and rotational zone. The simulation is conducted by taking into account a control volume around the wind turbine and determining the effective parameters such as boundary conditions in Fluent software. The velocity at the inlet of the control volume is constant and equal to the free-flow velocity. In this study, the inlet velocity is considered as 7 m/s. The air is considered as working fluid with a constant density of  $1.225 \text{ kg/m}^3$  and a constant viscosity of  $1.7894 \times 10^{-5} \text{ kg/ms}$ . Upwind second order method is used for discretization of continuity equations, momentum, kinetic energy of turbulence and loss of turbulence. In addition, SIMPLE algorithm is applied for pressure-velocity coupling. The convergence criteria are considered to be less than  $10^{-6}$  for all equations. Also, the SST  $k-\omega$  turbulence model which has high accuracy for simulating the flow around wind turbine blades is used.

#### 4. Grid Independency Study and Validation

In this study, four different grids with cell numbers of 95711, 236243, 454391 and 775041 is generated to calculate the torque in terms of tip speed ratio of the blade, respectively. Finally, in order to save time on the calculation, the grid with a cell number of 454391 is more suitable to obtain the results than other grids. Figure 5 indicates the detail of grid independency.

In order to validate the correctness of the simulation, numerical results should be compared with the experimental results. By doing this, the process of resolving is valid and can be ensured the results. For this purpose, the results of calculating the torque coefficient in terms of tip speed ratio of the present study when  $Re/m=4.32 \times 10^5$  and  $s/d=0.1$  are compared with the experimental results of Blackwell et al. [15]. As can be seen in Figure 6, the numerical results of the present study has a good agreement with experimental results and has a average error about 10%, so we can ensure the accuracy of the numerical results of this study.

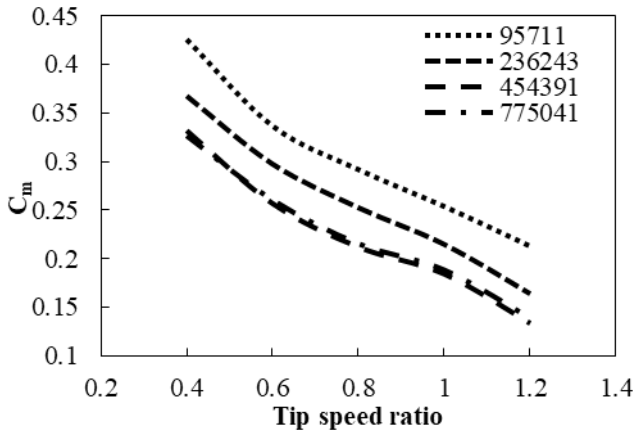


Figure 5. The grid independency study

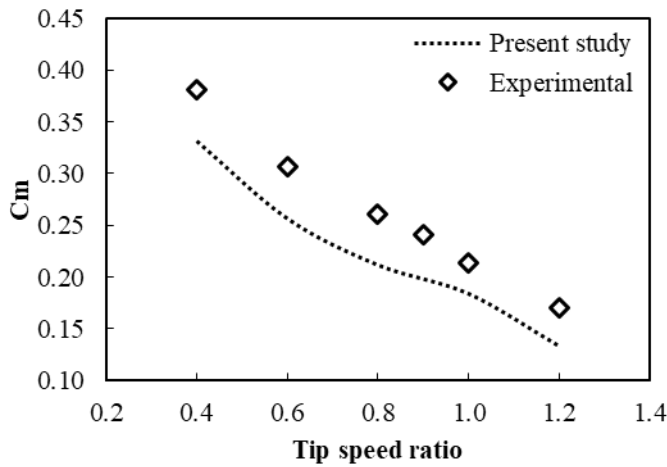


Figure 6. Comparison of the torque coefficient in terms of tip speed ratio of the present study with the experimental results of Blackwell et al. [15]

## 5. Results and Discussion

### 5.1. Effect of Overlap Ratio ( $s/d$ ) on Torque Coefficient and Power Coefficient

Figure 7 shows the changes of the torque coefficient in terms of tip speed ratio of the blade for two overlap ratios of 0.1, 0.2 and the case without overlap ratio. As can be seen, the lowest value of torque coefficient is obtained for overlap ratio of 0.2, so that for overlap ratio of 0.1 the torque coefficient is decreased about 45% when  $\lambda=1$  compared to overlap ratio of 0.1 and the torque coefficient is decreased about 22% when  $\lambda=1$  to the case without overlap ratio. Also, by increasing the tip speed ratio of the blade, the value of torque coefficient is decreased by a large slope, which indicates that in lower values of  $\lambda$ , there is a more torque than in higher values of  $\lambda$ . The reason for this is that by increasing the angular velocity of the turbine rotor, the value of turbine torque dramatically decreases. In Figure 8, the changes of the power coefficient in terms of tip speed ratio of the blade are shown for two overlap ratios ( $s/d$ ) of 0.1 and 0.2. As it is obvious, the maximum value of the power coefficient for overlap ratio of 0.1 is greater than the maximum value of the power coefficient for overlap ratio of 0.2 and the case without overlap ratio. The maximum value of the power coefficient for overlap ratio of 0.1 is equal to 0.1842 and for

overlap ratio of 0.2 is equal to 0.127 and for overlap ratio of 0 is equal to 0.155 when  $\lambda=1$ .

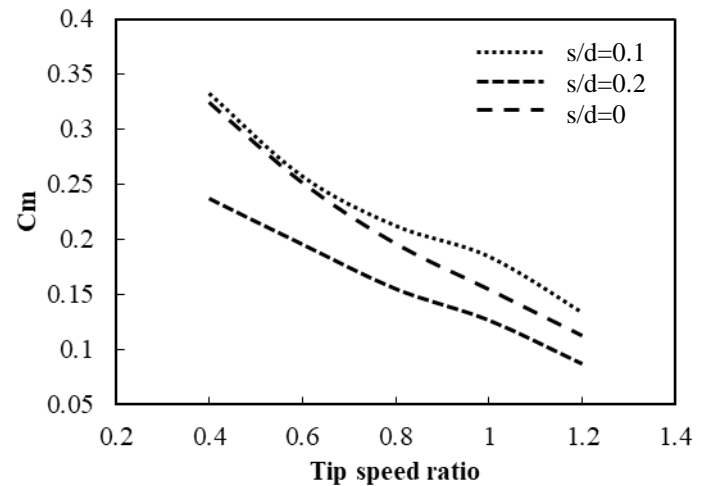


Figure 7. Comparison the effect of overlap ratio ( $s/d$ ) on torque coefficient in terms of tip speed ratio of the blade

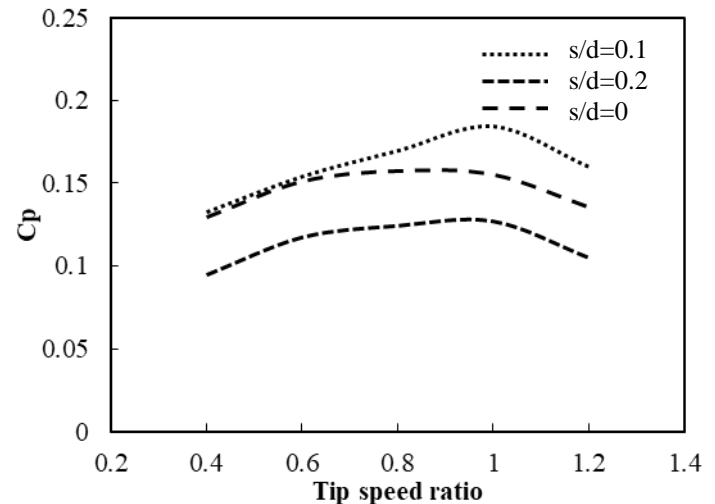


Figure 8. Comparison the effect of overlap ratio ( $s/d$ ) on power coefficient in terms of tip speed ratio of the blade

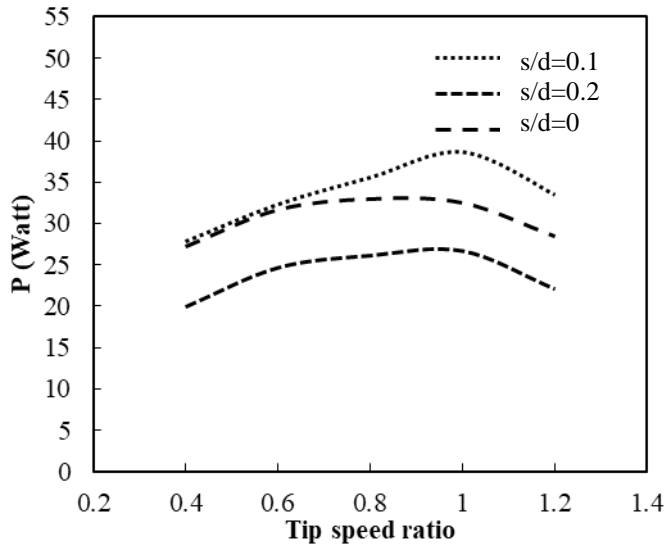
### 5.2. Effect of Overlap Ratio ( $s/d$ ) on Turbine Power

Figure 9 shows the changes of the power in terms of tip speed ratio of the blade for two overlap ratios ( $s/d$ ) of 0.1 and 0.2 and the case without overlap ratio. As can be seen, the maximum value of power is obtained for all three cases when  $\lambda=1$ . For overlap ratio of 0.1, the maximum value of turbine power is 38.7 watts, which is about 20% more than the case without overlap ratio when  $\lambda=1$  and about 45% more than for overlap ratio of 0.2.

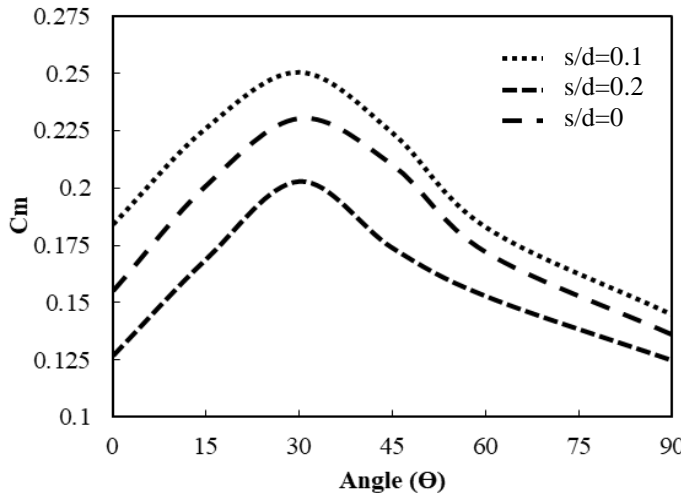
### 5.3. Effect of the Blade Angular Position ( $\Theta$ ) on Torque coefficient and Power Coefficient

Figure 10 demonstrates the changes of torque coefficient in terms of the blade angular position ( $\Theta$ ) of  $0^\circ$  to  $90^\circ$  for tip speed ratio value of 1. As can be seen, the highest peak of the torque coefficient is obtained at the angle of  $30^\circ$  for all overlap ratios. Compared to the other overlap ratios, it is obvious that overlap ratio of 0.1 has a remarkable and positive effect on torque coefficient.





**Figure 9.** Comparison of the effect of overlap ratio ( $s/d$ ) on the power in terms of the tip speed ratio of the blade



**Figure 10.** Comparison of the torque coefficient in terms of the blade angular position for  $\lambda = 1$

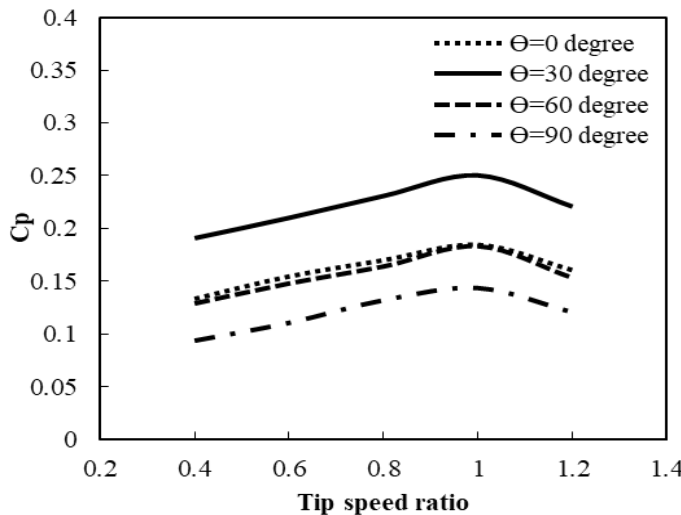


**Figure 11.** Comparison of the effect of blade angular position ( $\Theta$ ) on power coefficient in terms of the tip speed ratio for overlap ratio of 0.1

Figures 11 shows the changes of power coefficient in terms of tip speed ratio for different blade angular position values. In this figure, the maximum value of the power coefficient for overlap ratio of 0.1 and blade angular position of  $30^\circ$  is obtained 0.2503 when  $\lambda=1$ . These computations demonstrate that the value of power coefficient is increased about 45% compared to the blade angular position of  $0^\circ$ . Apart from that, the results for  $\Theta$  equal to  $0^\circ$  is similar to the results for that of  $60^\circ$ . Also, by increasing the blade angular position to  $90^\circ$ , the power coefficient reaches to the lowest value ( $C_p=0.144$ ).

### 5.3. Pressure Distribution Around the Turbine Blades

Figure 12 shows the pressure distribution (Pa) around the turbine blades in three-dimensional and two-dimensional views for overlap ratio of 0.1 which has the maximum value of power. As can be seen, when the flow moves to the inside and the buckets of the turbine blades, there is a higher value of pressure which this increasing of pressure using available energy in the wind causes to move the turbine blades and rotate its rotor. The maximum pressure values are seen in the convex side of the turbine blades, and there is a negative pressure region in the concave side of the turbine blades that this difference in the pressure of the convex and concave sides causes to rotate the wind turbine.

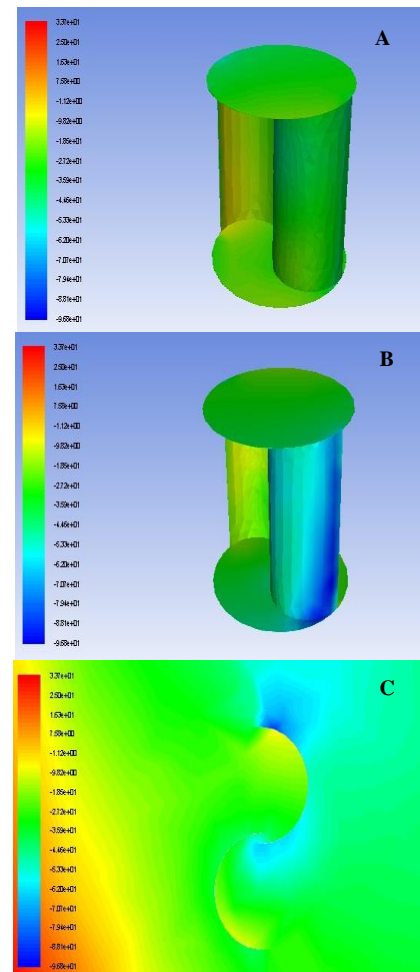


**Figure 12.** Pressure distribution (Pa) A) The front side of wind turbine B) The back side of wind turbine C) two-dimensional view for overlap ratio of 0.1

## 6. Conclusion

In this study, the effect of both overlap ratio of the blades and blade angular position on the performance of a savonius vertical axis wind turbine are investigated with computational fluids dynamics method. For this purpose, the computations are conducted for the wind turbine with overlap ratios of 0, 0.1 and 0.2. Also, the blade angular position varies from  $0^\circ$  to  $90^\circ$  in order to consider the effect of these parameters on the changes of torque coefficient and power coefficient around the blades of savonius wind turbine. The wind speed is 7 m/s and the flow is considered as three-dimensional, incompressible and turbulence. The results show that SST k- $\omega$  turbulence model is a suitable model for simulating the flow around the blade of savonius vertical axis wind turbine and it is in good agreement with the experimental results. It is also concluded that the value of torque coefficient is decreased by increasing of overlap ratio. In fact, the value of overlap ratio can be increased to an acceptable limit which in this study up to overlap ratio of 0.1 had a favorable result so that for overlap ratio of 0.1. The torque coefficient decreases about 45% when  $\lambda=1$  compared to overlap ratio of 0.1 so that the maximum value of the power coefficient for overlap ratios of 0.1, 0.2 and 0 is equal to 0.1842, 0.127 and 0.155 when  $\lambda=1$ , respectively. It is observed that the maximum value of power coefficient and torque coefficient is obtained for overlap ratio) of 0.1 for  $\lambda=1$ . The highest peak of the torque coefficient is obtained at the blade angular position of  $30^\circ$  for all overlap ratios. Also, the maximum value of the power coefficient for overlap ratio of 0.1 and blade angular position of  $30^\circ$  is obtained 0.2503 at  $\lambda = 1$  which is 45% more than that of  $0^\circ$ . The other obtained results from are as follows

- 1- By increasing the tip speed ratio of the blade, the value of torque coefficient is decreased by a large slope which in lower values of  $\lambda$ , there is a more torque than in the higher values of  $\lambda$ .
- 2- In the overlap ratio of 0.1, the torque coefficient is more than for overlap ratio of 0.2.
- 3- For overlap ratio of 0.1, the maximum value of turbine power is 38.7 watts, which is about 20% more than the case without overlap ratio for  $\lambda=1$  and about 45% more than for overlap ratio of 0.2.
- 4- The maximum pressure values are seen in the convex side of the turbine blades, and there is a negative pressure region in the concave side of the turbine blades.

## References

- [1] A.C. Chinchore, Computational Study of Savonius Wind Turbine. Diss. Cleveland State University, 2013.
- [2] N.H. Mahmoud, A.A. El-Haroun, E. Wahba, M.H. Nasef, An experimental study on improvement of Savonius rotor performance, Alexandria Engineering Journal 51 (2012) 19–25.
- [3] I. Ushiyama, H. Nagai, Optimum design configurations and performance of Savonius rotors, Wind Engineering (1988) 59–75.
- [4] L.F. Rus, Experimental study on the increase of the efficiency of vertical wind turbines by equipping them with wind concentrators, Journal Sustainable Energy 3 (2012) 30–35.
- [5] I.B. Alit, R. Susanto, I.M. Mara, M. Mirmanto, Effect of concentrator, blade diameter and blade number on the Savonius wind turbine performance, Asian Journal Applied Sciences 5 (2016) 343–351.
- [6] T.K. Aldoss, Savonius rotor using swinging blades as an augmentation system, Wind Engineering 8 (1984) 14–20.
- [7] T.K. Aldoss, Y.S.H. Najjar, Further development of the swinging-blade Savonius rotor, Wind Engineering 9 (1985) 65–70.
- [8] S.A. Tabassum, S.D. Probert, Vertical-axis wind turbine: a modified design, Applied Energy 28 (1987) 59–67.
- [9] P. Reupke, S.D. Probert, Slatted-blade Savonius wind-rotors, Applied Energy 40 (1991) 65–75.
- [10] T.T. Ogawa, Yoshida HH, Yokota YY. Development of Rotational Speed Control Systems for a Savonius-Type Wind Turbine. ASME. J. Fluids Eng. 111 (1989) 53–58.
- [11] U. K. Saha, M. Jaya Rajkumar, On the performance analysis of Savonius rotor with twisted blades, Renewable energy 31 (2006) 1776–1788.
- [12] U.K. Saha, P. Mahanta, A.S. Grinspan, P.S. Kumar, P. Goswami, Twisted bamboo bladed rotor for Savonius wind turbines, Journal of the Solar Energy Society of India (SESI) 4 (2005) 1–10.
- [13] B. Deb, R. Gupta, R.D. Misra, Performance analysis of a Helical Savonius rotor without shaft at  $45^\circ$  twist angle using CFD, Journal of Urban and Environmental Engineering 7 (2013) 126–133.
- [14] A. Damak, Z. Driss, M.S. Abid, Experimental investigation of helical Savonius rotor with a twist of  $180^\circ$ , Renewable Energy 52 (2013) 136–142.
- [15] B.F. Blackwell, R. F. Sheldahl, L. V. Feltz, Wind tunnel performance data for two-and three-bucket Savonius rotors. Springfield, VA, USA: Sandia Laboratories (1977) 1–105.
- [16] M. Cai, E. Abbasi, H. Arastoopour, Analysis of the performance of a wind-turbine airfoil under heavy-rain conditions using a multiphase computational fluid dynamics approach, Industrial & Engineering Chemistry Research 52 (2012) 3266–3275.
- [17] A.C. Cohan, H. Arastoopour, Numerical simulation and analysis of the effect of rain and surface property on wind-turbine airfoil performance, International Journal of Multiphase Flow 81 (2016) 46–53.
- [18] M. Islam, D. S-K. Ting, A. Fartaj, Aerodynamic models for Darrieus-type straight-bladed vertical axis wind turbines, Renewable and Sustainable Energy Reviews 12 (2008) 1087–1109.
- [19] Md F. Ismail, K. Vijayaraghavan, The effects of aerofoil profile modification on a vertical axis wind turbine performance, Energy 80 (2015) 20–31.
- [20] T. Chitsomboon, Ch. Thumthae, Adjustment of k-w SST turbulence model for an improved prediction of stalls on wind turbine blades, World Renewable Energy Congress-Sweden, Linköping; Sweden. No. 057. Linköping University Electronic Press, 8–13 May (2011).
- [21] A. Le Pape, J. Lecanu, 3D Navier–Stokes computations of a stall-regulated wind turbine, Wind Energy 7 (2004) 309–324.
- [22] M.H. Nasef, W.A. El-Askary, A.A. AbdEL-Hamid, H.E. Gad, Evaluation of Savonius rotor performance: Static and dynamic studies, Journal of Wind Engineering and Industrial Aerodynamics 123 (2013) 1–11.
- [23] F.R. Menter, Two-equation eddy-viscosity turbulence models for engineering applications, AIAA journal 32 (1994) 1598–1605.
- [24] H. Flores-Saldaña, A. Gallegos-Muñoz, N.C. Uzarraga-Rodriguez, V.H. Rangel-Hernandez, Numerical Analysis of the Overlap Effect Between Blades at Four-Bladed Rooftop VAWT, In ASME 2012 6th International Conference on Energy Sustainability collocated with the ASME 2012 10th International Conference on Fuel Cell Science, Engineering and Technology, American Society of Mechanical Engineers, (2012) 1341–1348.